# Dynamic Model of a Bubbling Fluidized Bed Boiler

Tuomas Kataja,
*Tampere University of Technology*
*Institute of Automation and Control*
*P.O. Box 692, FI-33101 TAMPERE*
*tuomas.kataja@tut.fi*

Yrjö Majanne
*Tampere University of Technology*
*Institute of Automation and Control*
*P.O. Box 692, FI-33101 TAMPERE*
*yrjo.majanne@tut.fi*

## Abstract

*A dynamic model for a high-volatile solid fuel fired bubbling fluidized bed boiler is presented. The model consist of an air-flue gas model which includes a furnace model describing combustion in a bubbling fluidized bed and a model for a water-steam circuit describing heat transfer from hot flue gases to water and steam. The versatile furnace model takes account of quality parameters of fuel so that the effects of moisture, particle size, heat value, and the amount of volatiles can be simulated. The model is based on the first principles mass, energy, and momentum balances. Results from validation of the model against a bubbling fluidized bed boiler process data are presented. The validation showed that the model can describe the dynamics and static gains of the process very well.*

**Keywords**: Dynamic boiler model, bubbling fluidized bed combustion.

## 1. Introduction

In the modern power generation the dynamic performance of power plants plays a very important role. This is because of the stringent demands of productivity and deregulation of energy markets. E.g. the increasing number of uncontrolled wind turbines connected to the power system disturbs the power balance which must be compensated by other controlled power plants. Also in process industry unit sizes of steam consuming processes, like paper machines have been increased causing bigger load disturbances for industrial power plants.

The most typical way to get information about the dynamic properties of the boiler is to perform test runs to determine e.g. thermal inertia, storage capacity, and load change rate. However, it is quite common that it is not possible to perform all the useful test runs because of the economic, productive, or safety reasons.

The other way to study the dynamic properties of the boilers is simulation. Mathematical modeling of boilers has been interested researchers already for decades [Maffezzoni, 1992]. Some of the pioneering works in this field are the works of Chien [Chien et al, 1958] and Profos [Profos, 1962]. The reported boiler models can be divided into two categories; fairly complicated models and simpler models derived for some limited purposes. The complicated models typically include dozens of nonlinear dynamic equations, static equations, variables and parameters. Some examples of those complicated models can be found e.g. in [Cori and Busi, 1977] and [McDonald and Kwatny, 1970]. In the simpler models many dynamic equations are neglected and many variables are not included. These models are typically applied to control purposes (design and implementation of model based control methods). Examples of this type of models are e.g. [Åström and Bell, 1998, 2000], [Cheres, 1990] and

[de Mello, 1991]. Most of these models are focused on the modeling of the water-steam cycle of the boiler, heat transfer from the furnace and the flue gas duct to the water-steam circuit, thermo hydraulics, flow dynamics, etc.

In the boiler models the phenomena in the furnace have been typically left for the minor consideration. The heat power released in the furnace is often handled as a simple first order transfer function from the fuel power demand. With this kind of approach it is not possible to take account the effect of fuel quality parameters to the operation of the boiler. However, especially with biomass fired boilers the quality of fuel may vary remarkably influencing on the performance and usability of the boiler. There is a lot of research work going on about the modeling of combustion of different type of fuels in different type of combustors, e.g. [Scala, 2002] and [Galgano, 2005]. However, the combustion models developed there are seldom connected with the dynamic boiler models. Some reasons for this may be that the combustion models require heavy computing and also it is the different research groups working with combustion models and boiler models and there is a lack of information transfer between these research areas.

The bubbling fluidized bed boiler model presented in this paper is developed in a research project with a boiler manufacturer Metso Power Inc. A moderately complicated combustion model is connected with the water-steam cycle model resulting a dynamic boiler model taking account also physical phenomena existing in the bubbling fluidized bed combustion. The model structure is described and some simulation results and future plans are depicted.

## 2.   Boiler Model

A dynamic model for the high-volatile solid fuel fired bubbling fluidized bed boiler consists of air-flue gas cycle (air preheaters, furnace, and heat exchangers) and water-steam cycle (water preheaters, drum, evaporator, super heaters, and steam attemperation). In addition steam pressure, steam temperature, and feed water control loops are included in the model. The simulator is built with MathWorks Inc's MATLAB/Simulink software. The model is based on the mass, energy, and momentum balances together with constitutional equations.

### 2.1   Air - Flue Gas Cycle

The furnace is divided into four segments according to the different combustion zones: the bed, the splashing region, the secondary zone, and the freeboard. The structure of the furnace model is shown in fig. 1. The fluidized bed is modeled according to the two-phase theory. In the theory the flow rate through the emulsion phase is equal to the flow rate for the minimum fluidization. Any flow in excess of that required for minimum fluidization appears as bubbles in the separate bubble phase [Toomey and Johnstone, 1952], [Oka, 2004], [Yang, 2003]. The bed is considered isothermal where two phases have uniform temperature. Minimum fluidization velocity is adopted from [Wen and Yu, 1966]. An average bubble size is assumed throughout the bed and calculated according to [Darton *et al.,*1977].

It is assumed that fuel is fed above the bed and it will spread uniformly and immediately across the cross-section of the bed. In the bed section, according to the two-phase theory, combustion takes place in the emulsion phase. Coarse char and fine char particles are burnt there. In the model the coarse char particles can also burst to the secondary zone of the furnace and drop back into the bed. The fine particles can elutriate out from the furnace [Galgano, 2005] and [Scala, 2002]. The elutriation constant for fine char particles is calculated according to [Tasirin and Geldart, 1998].

The rate of combustion is calculated by taking into account diffusive resistance to coarse char particles and kinetic resistance to elutriable size fine particles. Combustion rates depend also on the density and the diameter of the particle and oxygen concentration in the emulsion phase [Borman, 1998]. The fragmentation of fuel particles accelerates the combustion [Raiko, 2005]. The primary fragmentation occurs immediately when the particles arrive at the bed. Attrition and fragmentation by percolation increase the amount of the elutriable size fine char particles. For high volatile biomass, the generation of the fines is proportional to the coarse char combustion rate at the particle surface [Salatino, 1998]. For biomass the average diameter of the fine particles is assumed to be constant, 100 μm [Galgano, 2005]. Devolatilization occurs in the bed section and volatile components burn in the upper zone of the furnace. Devolatilization yields carbon monoxide, carbon dioxide, and hydrogen. The rate of devolatilization is modeled by a simple correlation considering diameter of the fuel particle and

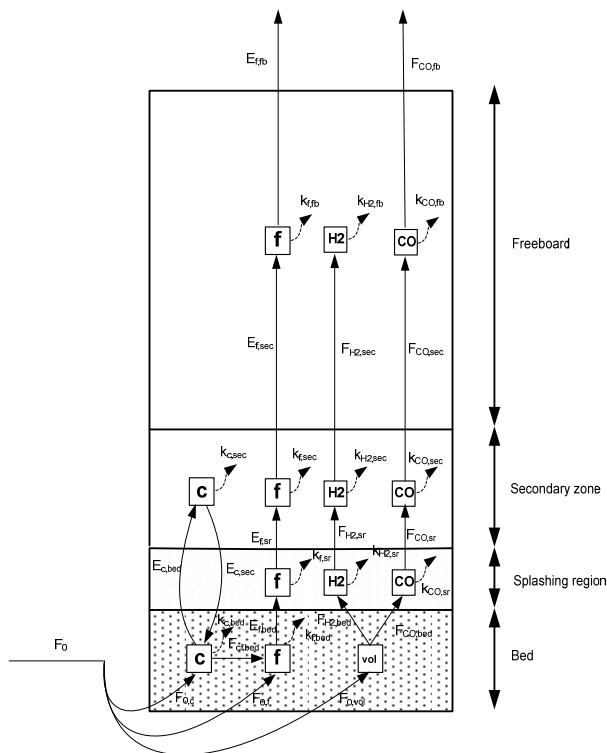temperature of the fluidized bed [de Diego, 2003], [Scala, 2002].



**Figure 1.** Structure of the furnace model. $F_0$ = fuel feed, **C** = coarse char balance equations, **f** = fine char particles balance equations, **vol** = volatile matter balance equations, **H2** = hydrogen balance equations, **CO** = carbon monoxide balance equations, E = entrainment of char coal from one zone to another zone, F = mass flow between model zones, k = burning rate of the material.

Heat transfer into the walls in the bed section is efficient. The heat transfer coefficient is modeled using the packet-renewal model [Mickey and Fairbanks, 1955], [Basu, 2006]. In the model the packets stay in contact with the wall surface short time and then sweep back to the bed. While the packet is in contact with the wall, the unsteady state heat transfer takes place between the packet and the surface.

Inert sand particles are ejected from the surface of the bed into the splashing region. The mass flow is calculated according to [Pemberton and Davidson, 1986]. Gas flows leaving the bubble and emulsion phases are assumed to be instantaneously mixed at a beginning of the splashing region [Okasha, 2007]. A clustering of bed particles is

neglected [Benoni, 1994]. The upper edge of the splashing region is assumed to be at the same level with a refractory wall of the furnace and the lower edge depends on the bed height. In the splashing region, all available oxygen reacts with carbon monoxide and hydrogen. Combustion of elutriated fines is assumed to be neglected. Heat transfer is modeled by the packet-renewal model.

Secondary air is brought to the secondary zone where the combustion of elutriated fines and volatiles takes place. Tertiary air is brought to the freeboard where some of the elutriated fines and volatiles are burned. Part of the elutriated fines and carbon monoxide can exit the furnace but hydrogen will burn out. In the secondary zone and the freeboard sections heat is transferred to the walls by radiation.

The furnace model is based on the time-depend ordinary differential mass and energy balance equations. The mass balances of fine char particles and oxygen are written in all furnace zones. It is assumed that average velocity of the fine particles equals to gaseous components. In addition in the bed section the mass balances are written for coarse char particles, volatile matter, and bursting sand particles. Energy balances are written for the hot coarse char particles and the bed including sand particles, fine char and gaseous components. It is assumed that the fine char particles are in the same temperature with the bed. The mass balance of the coarse char particles is also defined in the secondary zone.

**_Table 1._** *Mass and energy balances of the bed and the splashing region*

| | |
|---|---|
| _Balances of the bed:_ | _Balances of the splashing region:_ |

_Balances of the bed:_

Mass balance for the fine char particles:

$$\frac{d}{dt}W_{f,bed} = F_{0,f} + G - k_{f,bed}W_{f,bed} - k_{el} \tag{1}$$

Mass balance for the coarse char particles:

$$\frac{d}{dt}W_{c,bed} = F_{0,c} + E_c^{in} - G - $$
$$k_{c,bed}W_{c,bed} - E_c^{out} \tag{2}$$

Mass balance for the volatile matter:

$$\frac{d}{dt}W_{vol,bed} = F_{0,vol} - k_d W_{vol,bed} \tag{3}$$

Mass balance for the oxygen in the emulsion phase:

$$Ah_{mf}\varepsilon_{mf}\frac{d}{dt}C_{O2}^{bed} = Au_{mf}C_{O2}^{in} + \delta_B AK_{be}\Omega - $$
$$\frac{l}{M_C}\left(k_f W_{f,bed} + k_c W_{c,bed}\right) - Au_{mf}C_{O2}^{bed} \tag{4}$$

Mass balance for the sand:

$$\frac{d}{dt}W_{s,bed} = E_{s,sr} - E_{s,bed} \tag{5}$$

Energy balance for the coarce char particles:

$$c_C \frac{d}{dt}\left[\left(W_{c,bed} + W_{vol,bed}\right)\left(T_c - T_{ref}\right)\right] = F_{0,c}c_c\left(T_0 - T_{ref}\right) - Gc_c\left(T_c - T_{ref}\right) + $$
$$k_{c,bed}\frac{W_{c,bed}}{M_C}M_{O2}c_{O2}\left(T_{bed} - T_{ref}\right) - k_{c,bed}\frac{W_{c,bed}}{M_C}M_{CO2}c_{CO2}\left(T_c - T_{ref}\right) - $$
$$k_d W_{vol,bed}\Delta H_{vol} + H_v F_0\left(T_0 - T_{vap}\right) - H_v F_0 l + k_{c,bed}W_{c,bed}\Delta H_C - $$
$$\frac{6\left(W_{c,bed} + W_{vol,bed}\right)}{\rho_c d_c}\left[\alpha_{c,bed}\left(T_c - T_{bed}\right) + \sigma\varepsilon_{eff}\left(T_c^4 - T_{bed}^4\right)\right] \tag{6}$$

Energy balance for the bed sand and fine char particles:

$$\frac{d}{dt}\left[\left(W_{f,bed}c_f + W_s c_s\right)\left(T_{bed} - T_{ref}\right)\right] = F_{0,f}c_f\left(T_0 - T_{ref}\right) + $$
$$Gc_c\left(T_0 - T_{ref}\right) - k_{el}c_f\left(T_{bed} - T_{ref}\right) + w_{g,ap}c_g\left(T_0 - T_{bed}\right) + $$
$$k_c\frac{W_c}{M_C}M_{CO2}c_{CO2}\left(T_{bed} - T_{ref}\right) + \frac{k_f}{M_C}M_{CO2}c_{CO2}\left(T_{bed} - T_{ref}\right) - $$
$$\frac{k_f}{M_C}M_{O2}c_{O2}\left(T_{bed} - T_{ref}\right) + E_{s,sr}c_s\left(T_s - T_{bed}\right) + $$
$$k_d W_{vol,bed}c_{vol}\left(T_{vol} - T_{bed}\right) + $$
$$H_v F_0 c_{H2O}\left(T_{vap} - T_{bed}\right) + k_f W_{f,bed}\Delta H_f - Q_{bed} + $$
$$\frac{6\left(W_{c,bed} + W_{vol,bed}\right)}{\rho_c d_c}\left[\alpha_{c,bed}\left(T_c - T_{bed}\right) + \sigma\varepsilon_{eff}\left(T_c^4 - T_{bed}^4\right)\right] + $$
$$\sigma A\phi_{bedsr}\left(T_{sr}^4 - T_{bed}^4\right) \tag{7}$$

_Balances of the splashing region:_

Mass balance of the fine char particles:

$$\frac{d}{dt}W_{f,sr} = k_{el} - k_{f,sr}W_{f,sr} - \frac{u_{sr}}{h_{sr}}W_{f,sr} \tag{8}$$

Mass balance of the hydrogen:

$$Ah_{sr}\frac{d}{dt}C_{H2}^{sr} = k_d W_{V,bed}\frac{x_{H2}}{M_{H2}} - Ah_{sr}k_{H2,sr} - Au_{sr}C_{H2}^{sr} \tag{9}$$

Mass balance of the carbon monoxide:

$$Ah_{sr}\frac{d}{dt}C_{CO}^{sr} = k_d W_{V,bed}\frac{x_{CO}}{M_{CO}} - Ah_{sr}k_{CO,sr} - Au_{sr}C_{CO}^{sr} \tag{10}$$

Mass balance of the oxygen:

$$Ah_{sr}\frac{d}{dt}C_{O2}^{sr} = N_{O2}^{in} - \frac{k_f W_{f,sr}}{M_C} - \frac{Ah_{sr}}{2}\left(k_{CO,sr} + k_{H2,sr}\right) - Au_{sr}C_{O2}^{sr} \tag{11}$$

Mass balance of the water vapor:

$$Ah_{sr}\frac{d}{dt}C_{H2O}^{sr} = N_{H2O}^{in} + Ah_{sr}k_{H2,sr} - Au_{sr}C_{H2O}^{sr} \tag{12}$$

Mass balance of the sand:

$$\frac{d}{dt}W_{s,sr} = E_{s,bed} - \frac{E_{s,sr}}{\tau_s} \tag{13}$$

Energy balance of the sand:

$$W_{s,sr}c_s\frac{d}{dt}T_s = \chi\alpha_{c,sr}\tau_s\left(T_{sr} - T_s\right) + W_{s,sr}c_s\left(T_{bed} - T_s\right) \tag{14}$$

Energy balance of the splashing region:

$$\frac{d}{dt}\left[\left(W_{H2}c_{H2} + W_{CO}c_{CO} + W_f c_f + W_{s,sr}c_s\right)\left(T_{sr} - T_{ref}\right)\right] = w_{g,bed}c_{g,bed}\left(T_{bed} - T_{sr}\right) + $$
$$k_{el}W_{f,bed}c_f\left(T_{bed} - T_{ref}\right) - u_{sp}\frac{W_{f,sr}}{h_{sr}}c_f\left(T_{sr} - T_{ref}\right) + \frac{k_f}{M_C}M_{CO2}c_{CO2}\left(T_{sr} - T_{ref}\right) - $$
$$\frac{k_f}{M_C}M_{O2}c_{O2}\left(T_{sr} - T_{ref}\right) + k_{CO,sr}Ah_{sr}M_{CO2}c_{CO2}\left(T_{sr} - T_{ref}\right) + $$
$$k_{H2,sr}Ah_{sr}M_{H2O}c_{H2O}\left(T_{sr} - T_{ref}\right) - k_{CO,sr}Ah_{sr}M_{CO}c_{CO}\left(T_{sr} - T_{ref}\right) - $$
$$k_{H2,sr}Ah_{sr}M_{H2}c_{H2}\left(T_{sr} - T_{ref}\right) - \frac{1}{2}\left(k_{H2,sr} + k_{CO,sr}\right)Ah_{sr}M_{O2}c_{O2}\left(T_{sr} - T_{ref}\right) + $$
$$\chi\alpha_{c,sr}\left(T_s - T_{sr}\right) + k_f W_{f,sr}\Delta H_f + \left(k_{CO,sr}\Delta H_{CO} + k_{H2,sr}\Delta H_{H2}\right)Ah_{sr} - $$
$$Q_{sr} + \sigma A\left[\phi_{bedsr}\left(T_{bed}^4 - T_{sr}^4\right) + \phi_{bedsec}\left(T_{sec}^4 - T_{sr}^4\right)\right] \tag{15}$$

In the splashing region the mass and energy balances of the sand particles are defined. Hydrogen, carbon monoxide, and the water vapor mass balances and fine char and gas energy balances are written for the splashing region, the secondary zone, and the freeboard. In table 1 is written mass and energy balance equations for the bed and splashing region sections. Similar are written for the secondary zone and the freeboard sections.

In the heat exchange section of the air – flue gas cycle the heat transfer into the super heaters, feed water preheaters, and air preheaters is calculated. Primary, secondary, and tertiary airs are heated by the air preheaters. In the air preheater model the mass and energy balances of the air and the energy balance of the preheater metal mass are calculated. A schematic diagram of the air-flue gas model is shown in fig. 2.
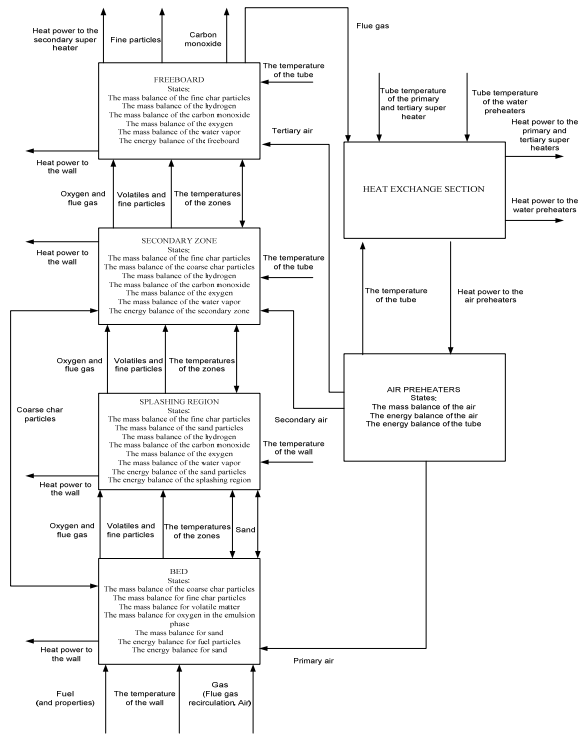
**Figure 2.** A schematic diagram of the air-flue gas model.

## 2.2 Water - Steam Cycle

In the evaporation circuit steam is generated inside the vertical tubes located on the furnace walls. Water-steam mixture flows up in a two-phase flow to the drum for phase separation [Adam & Marchetti, 1999].

In the model the evaporation circuit is divided into sixteen segments. Each wall is modeled separately and every wall is divided into four segments according to the furnace segments heights. It is assumed that the water-steam mixture is saturated. The energy balances are written for the water-steam mixture and for the furnace wall tubes. Energy balances for the refractory elements are also written for the two lowest segments of the evaporation circuit. The steam quality and the density of the water-steam mixture are calculated in every segment. Heat flux from the tube wall to the water-steam mixture is calculated by using an experimental equation [Ordys 1994].

Usually the heat flow from the furnace to the evaporator is assumed to be uniform [Åström 2000], [Kim 2005], but in this model the heat flow is divided into each evaporator segment (16 pc.)

according to the temperature of the furnace and the heat transfer coefficient in each zone.

Water-steam mixture in the drum is divided into water and steam sub-volumes interacting with each other. The mass balance equation is applied to both sub-volumes and the energy balance is applied to water sub-volume [Kim, 2005], [Ordys, 1994], [Åström, 2000]. From the drum steam is directed to the super heaters. Saturated water in the drum is mixed with feed water coming from the water preheaters. The incoming feed water is directed to the downcomers. In the naturally circulating drum type boilers density difference between the water in the downcomers and the two-phase mixture in the evaporation tubes is the driving force of the natural circulation.

The modeled boiler is equipped with three super heaters and two feed water preheaters. The super heaters are used to raise the live steam temperature. The temperature is controlled by steam attemperating sprays. The feed water preheaters are used to transfer low grade flue gas heat to feed water. The heat exchanger models are based on the mass, energy, and momentum balances. Heat is transferred into exchangers from the heat exchange section of the air-flue gas model. A schematic diagram of the water-steam model is shown in fig 3 and main mass and energy balance equations of the water - steam cycle is written in table 2.

**Table 2.** *Mass and energy balances of the water – steam cycle.*

*Balances of the evaporation circuit section:*

*Energy balance of the refractory wall in the bed section:*

$$m_{rf} c_{rf} \frac{d}{dt}(T_{rf}) = Q_{rf} - Q_{cond} \tag{16}$$

*Energy balance of the evaporation circuit in the one refractoty area section:*

$$V_{rf} \frac{d}{dt}(\rho_{wv} h_{wv,out}) = Q_{cond} + w_{wv,in} h_{wv,in} - w_{wv,out} h_{wv,out} \tag{17}$$

*Energy balance of the evaporation circuit in the one tube area section:*

$$V_t \frac{d}{dt}(\rho_{wv} h_{wv,out}) = Q_{in,ev} + w_{wv,in} h_{wv,in} - w_{wv,out} h_{wv,out} \tag{18}$$

*Balances of the drum section:*

*Mass balance of the drum water:*

$$\frac{d}{dt}(m_{dr}) = w_e + (1-x)w_{ev} - w_{dc} - w_{ec} \qquad (19)$$

*Energy balance of the drum water:*

$$\frac{d}{dt}(m_{dr}h_w) = w_e h_e + (1-x)w_{ev}h_w - w_{dc}h_w - w_{ec}h_v \qquad (20)$$

*Mass balance of the drum steam:*

$$\frac{d}{dt}(V_v\rho_v) = xw_{ev} - w_v - w_{ec} \qquad (22)$$

*Balances of the super heater section:*

*Energy balance of the steam in the one superheater section:*

$$V_{sh}\frac{d}{dt}(\rho_v h_{v,out}) = Q_{in,sh} + w_{v,in}h_{v,in} - w_{v,out}h_{v,out} \qquad (23)$$

*Energy balance of the tube in the one superheater section:*

$$m_{sh}c_{sh}\frac{d}{dt}(T_{sh}) = Q_{sh} - Q_{in,sh} \qquad (24)$$

*Mass balance of the steam in the one superheater section :*

$$\frac{d}{dt}(w_{v,in}) = \frac{w_{v,out} - w_{v,in}}{\tau_{sh}} \qquad (25)$$

*Balances of the feed water preheater section:*

*Energy balance of the feed water in the one feed water preheater section:*

$$V_e\frac{d}{dt}(\rho_e h_{e,out}) = Q_{in,e} + w_{e,in}h_{e,in} - w_{e,ou}h_{e,out} \qquad (26)$$

*Energy balance of the tube in the one feed water preheater section:*

$$m_e c_e \frac{d}{dt}(T_e) = Q_e - Q_{in,e} \qquad (27)$$
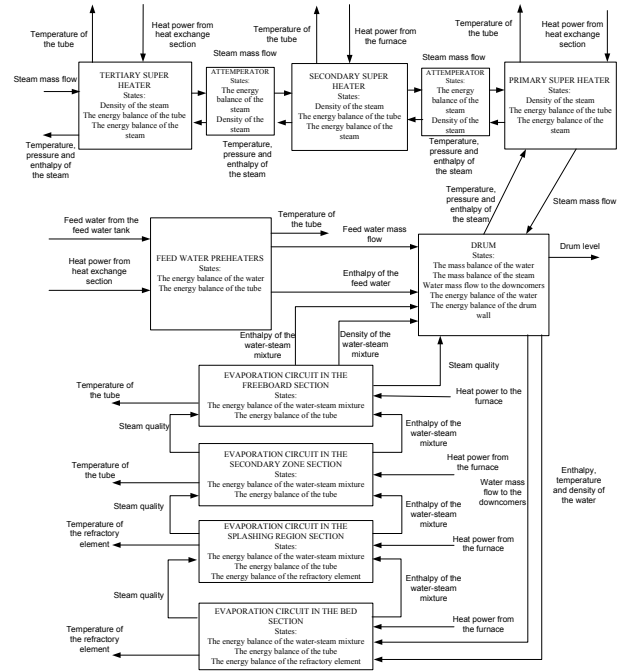


**Figure 3.** A schematic diagram of the water-steam model.

# 3. Comparisons with plant data and simulation tests

The model is parameterized using a construction data and measured process data from a 260 MW$_{th}$ bubbling fluidized bed boiler. The validation of the model showed that the model can describe the dynamics and the static gains of the process very well. The model is tested using measured process data as an input to the model and then compared the computed signals with the measured outputs. Figure 4 depicts the measured and simulated results of the drum pressure and the live steam pressure.

Figure 5 depicts simulated and measured fuel mass flows. In the model milled peat and bark are used as a fuel. Measured fuel mass flow is estimation from real fuel mass flow. Also the heat value and moisture of the fuel cannot be measured. Still results are quite close to each other.
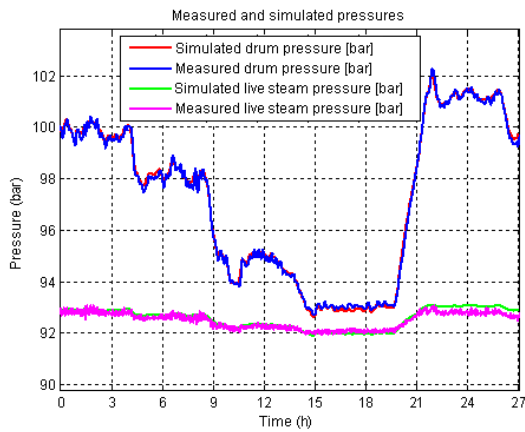
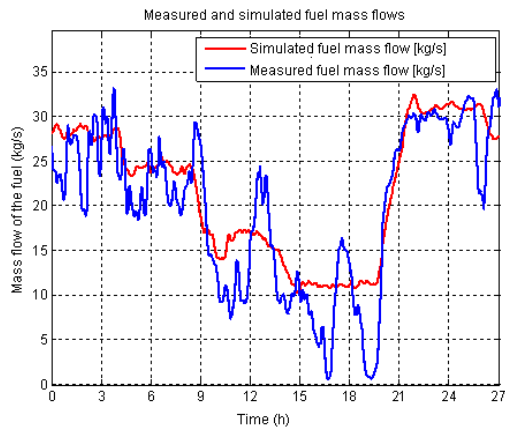**Figure 4.** Measured and simulated drum and live steam pressures.



**Figure 5.** Measured and simulated fuel mass flows.

The model is used to study the dynamic behavior of the boiler process. The points of interest are e.g. the thermal inertia and the steam storage capacity of the boiler. Knowledge about the behavior of these properties gives useful information for the process and control design. The dynamic model helps process developers to answer questions like how long a boiler can generate steam in case of a boiler trip or what will happen in the process during a black out situation?

Figure 6 depicts the boiler dynamic response when the fuel mass flow rate is increased 10 %. From the simulation results e.g. the time delay and the time constant of the boiler can be solved. In the test control loops are switched off.
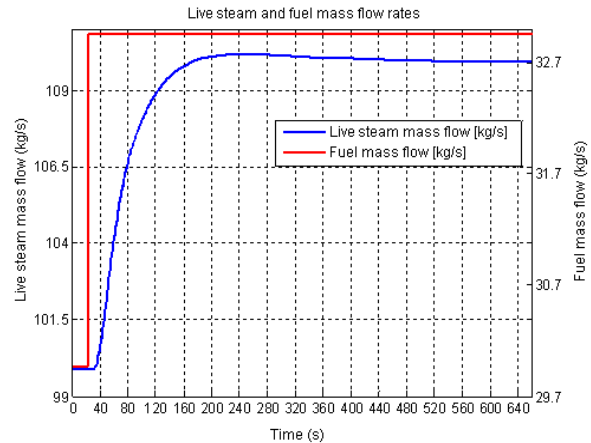


**Figure 6.** The response of the boiler to the 10 % fuel mass flow rate step change.
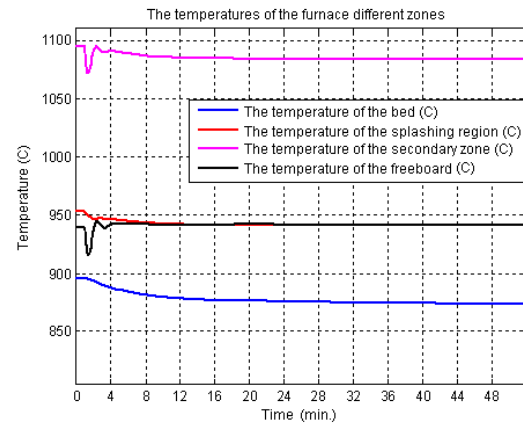


**Figure 7.** The step responses of the furnace temperatures in different zones when increasing the moisture of the fuel 10%.

In fig. 7 the dynamic behavior of the different zones of the furnace is studied when increasing the moisture content of the fuel 10 %. The control loops are switched on. The temperatures of the bed and the splashing region are dropped slowly due to the thermal capacity of sand.

## 4.    Conclusions and future plans

A dynamic model of the bubbling fluidized boiler is presented. The model is based on physical parameters for the boiler and can quite easily scale to represent any drum type BFB boiler. The model consists of the air-flue gas model and the water-steam circuit model. In the air-flue gas model furnace model takes into account important processes which effects on combustion dynamics like fuel particle fragmentation, attrition and volatile

matter segregation and post combustion in the upper zones. In the water-steam circuit model the dynamics of the steam generation in the evaporation circuit, separation of the steam in the drum section and super heating of the steam ar investigated. Also feed water preheater dynamics are studied.

The model is nonlinear and agrees well with experimental data. The model helps to study the dynamic behavior of the boiler process.

The future plans of the modeling project are to test the developed model by modeling three different size bubbling bed boilers and compare the simulated results with the measured data. Also the user interface of the simulator will be developed to make the build up of the simulator faster. There is also another project going on with Metso Power to develop a similar simulation model for a circulating fluidized bed boiler.

# Nomenclature

| | |
|---|---|
| $A$ | Cross-sectional area of the furnace [m$^2$] |
| $c_x$ | Specific heat of the component $x$ [kJ/kgK] |
| $C_x^y$ | Concentration of component $x$ in section $y$ |
| $d_x$ | Average diameter of component $x$ [m] |
| $E_x^z$ | Entrainment rate of the component $x$ to the direction $z$ [kg/s] |
| $F_{0,x}$ | Fuel feed mass flow rate of the component $x$ [kg/s] |
| $G$ | Fine particles generation constant [kg/s] |
| $h_{mf}$ | Height of the bed in the minimum fluidization velocity [m] |
| $H_v$ | Moisture content of the fuel [-] |
| $h_x$ | Enthalpy of component $x$ [kJ/kg] |
| $h_y$ | Height of the section $y$ [m] |
| $\Delta H_x$ | Heat of combustion of component $x$ [kJ/kg] or [kJ/kmol] |
| $K_{be}$ | Mass transfer coefficient between dense phase and bubbles [1/s] |
| $k_d$ | Devolatilization constant [1/s] |
| $k_{el}$ | Fines elutriation mass flow [kg/s] |
| $k_{x,y}$ | Combustion rate of component $x$ in section $y$ [s$^{-1}$] |
| $l$ | Latent heat [kJ/kg] |
| $M_x$ | Molecular weight of component $x$ [kg/kmol] |
| $m_y$ | Mass of the section $y$ [kg] |
| $N_x^z$ | Quantity mass flow of component $x$ to direction $y$ [mol/s] |

| | |
|---|---|
| $Q_{in,y}$ | Heat power from the tube to the fluid in the section $y$ [W] |
| $Q_y$ | Heat power to the wall in the section $y$ [W] |
| $T_x$ | Temperature of the component $x$ [K] |
| $u_{mf}$ | Minimum fluidization velocity [m/s] |
| $u_y$ | Gas velocity in section $y$ [m/s] |
| $V_y$ | Volume of the section $y$ [m$^3$] |
| $W_{x,y}$ | Mass of component $x$ in section $y$ [kg] |
| $w_y$ | Mass flow from section $y$ [kg/s] |
| $x$ | Steam quality [-] |
| $x_x$ | Mass fraction of component $x$ [-] |
| $\alpha_{x,y}$ | Heat transfer coefficient of component $x$ in section $y$ [W/Km$^2$] |
| $\delta_B$ | Bubble fraction in the bed [-] |
| $\varepsilon_{eff}$ | Effective emissivity [-] |
| $\varepsilon_{mf}$ | Voidage at minimum fluidization [-] |
| $\rho_x$ | Density of the component $x$ [kg/m$^3$] |
| $\sigma$ | Stefan-Boltzmann constant [W/m$^2$K$^4$] |
| $\tau_x$ | Residence time of component $x$ |
| $\phi_{xy}$ | View factor related to region $x$ and $y$ [-] |
| $\chi$ | Total exposed surface area of ejected inert particles [m$^2$] |
| $\Omega$ | Coefficient between dense phase and bubbles [-] |

## Subscripts and superscripts

| | |
|---|---|
| $ap$ | Air preheater |
| $bed$ | Bed |
| $C$ | Carbon |
| $c$ | Coarse char particle |
| $dr$ | Drum |
| $CO$ | Carbon monoxide |
| $CO2$ | Carbon oxide |
| $cond$ | Conduction |
| $d$ | Devolatilization |
| $dc$ | Downcomer |
| $e$ | Feed water preheater |
| $ec$ | Evaporation in the drum |
| $ev$ | Evaporation circuit |
| $f$ | Fine char particle |
| $g$ | Gas |
| $H2$ | Hydrogen |
| $H2O$ | Water in the combustion |

| | |
|---|---|
| *in* | Inlet direction |
| *O2* | Oxygen |
| *out* | Outlet direction |
| *ref* | Reference |
| *rf* | Refractory wall |
| *s* | Sand |
| *sh* | Super heater |
| *sec* | Secondary zone |
| *sr* | Splashing region |
| *t* | Tube |
| *v* | Steam |
| *vap* | Vaporization |
| *vol* | Volatile matter |
| *w* | Water |
| *wv* | Water-steam mixture |
| *0* | Initial |

# References

Adam EJ & Marchetti L. (1999). Dynamic simulation of large boilers with natural recirculation. Combust Chem Eng 1999;23:1031–40.

Basu, P. (2006). Combustion and gasification in fluidized beds. Boca Raton, CRC Press. 473 p.

Benoni, D., Briens, C. L., Baron, T., Duchesne, E., & Knowlton, T. M. (1994). A procedure to determine particle agglomeration in a fluidized bed and its effect on entrainment. Powder Technology, Vol 78, pp. 33-42.

Borman, G.L. & Ragland, K,W. (1998). Combustion engineering. Singapore, McGraw-Hill Inc. 613 p.

Cheres, E. (1990). Small and medium size drum boiler models suitable for long term dynamic response. IEEE Transactions on Energy Conversion, Vol. 5, No. 4, pp. 686–692

Chirone, R., Marzocchella, A., Salatino, P., Scala, F. (1999) Fluidized bed combustion of high-volatile solid fuels: An assessment of char attrition and volatile matter segregation, Proceedings of the 15th International Conference on Fluidized Bed Combustion, Savannah, May 16–19, 1999, The American Society of Mechanical Engineers, Paper No. FBC99-0021.

Chien, K. L., Ergin, E. I., Ling, C., &Lee, A. (1958). Dynamic analysis of a boiler. Transactions of ASME, 80, 1809–1819.

Cori, R., & Busi, T. (1977). Parameter identification of a drum boiler power plant. Proc. 3rd Power Plant Dynamics, Control and Testing Symposium, Knoxwille, Tennessee, September 7-9, 1977.

Darton, R.C., La Nauze, J-F., Davidson, J.F. & Harrison, D. (1977). Bubble growth due to coalescence in fluidized beds. Transactions of the Institution of Chemical Engineers, Vol 55, pp. 274-280.

de Diego, L.F., Garcia-Labiano, F., Abad, A., Gayan, P. & Adanez, J. (2003). Effect of moisture content on devolatilization times of pine wood particles in a fluidized bed. Energy & Fuels, Vol. 17, No.2, pp. 285-290.

Galgano, A., Salatino, P., Crescitelli, S., Scala, F. & Maffettone, P.L. (2005). A model of the dynamics of a fluidized bed combustor burning biomass. Combustion and flame Vol.140, No.4, pp. 271–284.

Kim, H. & Choi, S. (2005). A model on water level dynamics in natural circulation drum-type boilers. Heat and mass transfer, Vol. 32, pp. 786–796.

Maffezzoni, C. (1992). Issues in modeling and simulation of power plants. In Proceedings of IFAC symposium on control of power plants and power systems, Vol. 1, pp. 19–27

McDonald, J. P., & Kwatny, H. G. (1970). A mathematical model for reheat boiler–turbine–generator systems. In Proceedings of IEEE. PES winter power meeting, New York. Paper 70 CP221-PWR.

de Mello, F. P. (1991). Boiler models for system dynamic performance studies. IEEE Transactions on Power Systems, Vol 6, No. 1, pp. 753–761

Mickey, H.S. & Fairbanks, D.F. (1955). Mechanism of heat transfer to fluidized beds. AICHE J, Vol.1, pp. 374–384.

Oka, S. (2004). Fluidized bed Combustion. New York, Marcel Dekker, Inc. 590 p.

Okasha, F. (2007). Modeling combustion of straw-bitumen pellets in a fluidized bed. Fuel Processing Technology, Vol 88, pp. 281-293.

Ordys, A.W., Pike, A.W., Johnson, M.A., Katebi, R.M. & Grimble M.J. (1994). Modelling and Simulation of Power Generation Plants. London, Springer-Verlag. 311 p.

Pemberton, S. T., & Davidson, J. F. (1986). Elutriation from fluidized beds—I. Particle ejection from the dense phase into the freeboard. Chemical Engineering Science, Vol. 41, pp. 243-251.

Profos, P. (1962). Die Regelung von Dampfanlagen. Berlin: Springer.

Raiko, R., Saastamoinen, J., Hupa, M. & Kurki-Suonio, I. Poltto ja palaminen. 2nd ed. Jyväskylä 2002, Teknillistieteelliset akatemiat. 744 p.

Salatino, P., Scala, F. & Chirone, R. Proc. of 27th Symp (Int.) on Combust., Combustion Institute, Pittsburgh (PA) in press (1998)

Scala, F. & Chirone, R. (2006). Combustion and attrition of biomass in fluidized bed. Energy and fuels, Vol. 20, pp. 91-102.

Scala, F. & Salatino, P. (2002). Modelling fluidized bed combustion of high-volatile solid fuels. Chemical engineering science, Vol. 57, pp. 1175-1196.

Scala, F., Salatino, P. & Chirone, R. (2000). Fluidized bed combustion of biomass char (robinia pseudoacacia). Energy & Fuels, Vol. 14, No.4, pp. 781-790.

Tasirin, S.M & Geldart, D. (1998). Enrainment of FCC from fluidized beds – a new correlation for the elutriation rate constants $K_{i\infty}$. Powder Technology, Vol. 95, pp. 240-247.

Toomey, R.D. & Johnstone, H.F. (1952). Gaseous fluidization of solid particles. Chem Eng Prog, Vol. 48, pp. 220–226.

Wen, C.Y. & Yu, Y.W. (1966). Mechanics of fluidization. Eng. Progr. Symp. Series 100-125.

Yang, W-C. (2003). Handbook of fluidization and fluid-particle systems. New York. Marcel Dekker, Inc. 861 p.

Åström, K. J., & Bell, R. (1988). Simple drum-boiler models. In IFAC international symposium on power systems, modelling and control applications. Brussels, Belgium.

Åström, K. J., & Bell, R. (2000). Drum boiler dynamics. Automatica, 36, pp. 363–378